PHYSICAL REVIEW E **75**, 061107 (2007)

Fluctuation-induced phase transition in a spatially extended model for catalytic CO oxidation

M. Pineda,[1] L. Schimansky-Geier,[2] and R Imbihl[1]
[1]*Institut für Physikalische Chemie und Elektrochemie, Leibniz Universität Hannover, Callinstraße 3-3a, D-30167 Hannover, Germany*
[2]*Institut für Physik, Humboldt Universität zu Berlin, Newton Straße 15, D-12489 Berlin, Germany*

(Received 9 November 2006; revised manuscript received 25 March 2007; published 8 June 2007)

A reaction-diffusion master equation has been introduced in order to model the bistable CO oxidation on single crystal metal surfaces at high pressure where the diffusion length becomes small and local fluctuations are important. Analytical solutions can be found in a reduced one-component nonlinear master equation after applying the Weiss mean-field approximation together with the adiabatic elimination of oxygen. It is shown that the Weiss mean-field approximation predicts a symmetry-breaking bifurcation associated with a phase transition. The corresponding stationary solutions of the nonlinear master equation are supported by Gillespie-type Monte Carlo simulations.

DOI: 10.1103/PhysRevE.75.061107 PACS number(s): 05.40.−a, 82.65.+r

I. INTRODUCTION

Heterogeneous catalysis is an important part of chemical industry but it also finds applications in environmental chemistry and energy conversion [1]. The elementary processes of catalytic reactions are typically studied in surface science type experiments with single crystal surfaces as model catalysts. However, the workhorse of real catalysis is supported catalysts where small metal particles of a few nanometer size are supported on an oxidic support material. Due to the small number of reacting particles on such nanoscale systems internal fluctuations in the adsorbate coverage become important and this has been the motivation in the past to study these fluctuations experimentally and theoretically [2–5]. As proposed recently, such fluctuations may not only arise on nanoscale surfaces but also on macroscopic surface planes if we choose conditions which restrict the diffusion length of adsorbed particles such that again the number of reacting particles becomes sufficiently small [6]. In this publication we present an analysis of fluctuations in catalytic CO oxidation which applies to such a situation realized with a homogeneous catalytic surface at high enough pressure.

Fluctuations and fluctuation-induced phenomena have been studied theoretically in many systems. The constructive role of noise in these systems is well established. Phenomena like noise-induced patterns, stochastic resonances, and stochastic ratchets or Brownian motors are a few of the many examples which have been analyzed [7–9]. In heterogeneous catalysis stochastic resonances have been reported in models of catalytic CO oxidation and catalytic NO reduction on Pt surfaces [10,11]. The role of a ratchet potential in connection with an ac electrical field has been studied in connection with electromigration on stepped surfaces [12]. With field electron microscopy the behavior of coverage fluctuations in CO oxidation on a Pt field emitter tip was investigated, and it was shown that fluctuations induce transitions between the two stable kinetic stationary states that coexist in the bistable range [2,3]. By varying the diameter of Pd particles it was demonstrated by molecular beam experiments that bistability in catalytic CO oxidation vanishes below a critical particle size [4]. The influence of external noise has been studied experimentally and theoretically with catalytic CO oxidation on an Ir(111) surface [13,14].

In order to understand coverage fluctuations in surface reactions, various approaches have been formulated. Fluctuations are naturally present in kinetic Monte Carlo (KMC) type simulations, but this technique has the inherent disadvantage that the adsorbate mobilities are unrealistically low. For this reason hybrid models have been formulated which treat the fast diffusing species as a mean-field variable, whereas the slow diffusing species are simulated with the full KMC algorithm [15–18]. On the other hand, stochastic simulations of catalytic CO oxidation have also been carried out with mean-field equations using birth and death processes to include the effect of fluctuations [19].

KMC simulations are essentially numerical experiments and do not constitute an analytic theory. An analytical approach was recently undertaken with a master equation describing the catalytic CO oxidation on a nanoscale surface, where the reactants can be considered as well mixed [5]. It was shown analytically that coverage fluctuations induce transitions between the two stable kinetic stationary states of the bistable region.

The area, in which the reactants in catalytic CO oxidation can be considered as well mixed and which therefore can be represented by a single ordinary differential equation (ODE), is given by the diffusion length of CO. On an extended single crystal surface this area is macroscopic at low pressure, but with increasing pressure the area becomes smaller. The number of gas particles impinging on the surfaces grows proportional to the pressure and therefore the surface residence time τ of the adsorbate decreases with increasing pressure. Simultaneously the total adsorbate coverage will approach the saturation limit and, since surface diffusion requires vacant sites, the diffusion rate will become very low. Since the diffusion length is given roughly by $\sqrt{\tau D_{\mathrm{CO}}}$ the combined effect will lead to a smaller and smaller diffusion length with increasing pressure (D_{CO} is the diffusivity). Stochastic patterns ("raindrop patterns") observed in catalytic CO oxidation on Pt(110) at 10^{-2} mbar were interpreted in this way and simulations incorporating stochastic elements were able to reproduce this finding [6].

Here we propose the following approach to model the stochasticity of catalytic CO oxidation at high pressure on an extended homogeneous surface. We envision the surface as being composed of an array of small compartments with identical properties inside which the adsorbates are well mixed. These compartments are coupled via CO diffusion. Inside each cell the diffusion is assumed to be infinitely fast and therefore each cell is represented by an ODE, which describes the bistability of the reactive system but also allows for fluctuations. The whole array of cells is represented by a reaction-diffusion master equation (RDME) which permits local fluctuations [20]. This equation describes the evolution of the probability distribution function (PDF) for the number of adsorbed molecules. One disadvantage of this RDME is that an analytical solution is not available in general [21]. Nevertheless, this problem can be solved in part by introducing appropriate approximations. In this paper, we use the Weiss mean-field approach and the adiabatic elimination of fast variables [7,8].

With these two approximations, we are able to solve the RDME. These methods allow us to obtain a reduced RDME and to get theoretical expressions for the PDF of the CO coverage. In this way, we can construct the phase diagram of the model as predicted by the Weiss mean-field approximation. This allows us to study the dynamic behavior of the system depending on the cell size and on the coupling parameter between cells. We show evidence for a phase transition which is characterized by an ordered symmetry-breaking state. It is reflected by an abrupt change in the order parameter depending on the strength of internal fluctuations and the coupling parameter. Our theoretical results are compared with stochastic simulations based on the Gillespie algorithm using adiabatic elimination and the Weiss mean-field approach [22].

The paper is organized as follows. The general model is presented in Sec. II. The RDME for catalytic CO oxidation is derived in Sec. III. Section IV is devoted to applying the Weiss mean-field approximation to our RDME. The application of adiabatic elimination and the solution of the RDME is studied in Sec. V In Sec. VI the possibility of a phase transition in our bistable reaction model, as predicted by the Weiss mean-field approximation, is explored. Summary and conclusions are presented in Sec. VII.

II. STOCHASTIC REACTION-DIFFUSION MODEL

Catalytic CO oxidation is probably the most extensively studied reaction in the field of surface science [1]. The elementary steps of this reaction on noble metal surfaces such as Pt, Pd, and Rh are well established and consist of the following reactions:

$$\mathrm{CO(gas)} + * \rightarrow \mathrm{CO(ads)},$$

$$\mathrm{CO(ads)} \rightarrow \mathrm{CO(gas)} + *,$$

$$\mathrm{O_2(gas)} + 2* \rightarrow 2\mathrm{O(ads)},$$

$$\mathrm{CO(ads)} + \mathrm{O(ads)} \rightarrow \mathrm{CO_2(gas)} + 2*,$$

with * and (ads) denoting a vacant adsorption site and adsorbed molecules or adatoms, respectively [23,24].

On a macroscopically large Pt surface the reaction sequence shown above produces bistability. Two stable kinetic stationary states coexist on the parameter region of bistability. Without fluctuations the macroscopic rate laws predict that the system resides on one of two stationary stable states for an infinite period of time. Decreasing the surface size to nanoscale dimensions, fluctuations in the particle number increase and transitions between the two stable states are now possible. Until now most of the previous studies on fluctuations in surface reactions focused on the coverage fluctuations which develop in catalytic CO oxidation on well mixed nanoscale surfaces at low pressure. In this case the analysis is performed on a single $L\times L$ site square lattice [2–5,18,19].

However, in order to study stochastic effects under conditions of relative high pressure, a surface is divided into a square lattice of cells, which are at the same time regarded as well mixed and therefore are chosen to be smaller than the diffusion length. Each small cell is represented as a $L\times L = A$ square grid of adsorption sites and the reaction is described using the traditional eight-site model which was first introduced by James *et al.* [16]. Because we are working on a perfect single crystal surface, the cells exhibit equal catalytic activity (e.g., identical sticking coefficients). The model incorporates the following steps.

(i) CO(gas) adsorbs onto single empty sites at rate p_{CO}. CO(ads) hops very rapidly to other empty sites on the cell. We consider below the case of infinitely mobile CO(ads) inside each cell [16], and neglect energetic interactions between CO(ads) and other CO(ads) and O(ads) adparticles. This feature is important in order to produce the bistability observed in experiments. The distribution of CO(ads) on sites not occupied by O(ads) is random. CO(ads) desorbs from the surface at a rate d. The parameter d corresponds to the temperature in experiments, because CO desorption is the strongest activated step in the Langmuir-Hinshelwood (LH) sequence.

(ii) $\mathrm{O_2}$(gas) adsorbs dissociatively at diagonal nearest-neighbor (NN) empty sites at a rate proportional to $p_{\mathrm{O_2}}$, provided that the additional six sites adjacent to these sites are not occupied by O(ads). This "eight-site rule" reflects the very strong NN O(ads)-O(ads) repulsion of the (2×2) superlattice ordering observed on Pt(111) [25]. This limits the highest reachable oxygen coverage to 0.25. O(ads) is immobile in the T range considered here due to its large bonding energy, and it also cannot desorb.

(iii) Each adjacent pair of CO(ads) and O(ads) can react at rate k to form $\mathrm{CO_2}$, which is immediately released into the gas phase.

Here we are interested in high pressure conditions. The cells have to be well-mixed and their size at high pressure has to be chosen therefore to be of nanoscale dimensions. Consequently, the deterministic description breaks down and stochastic effects become relevant. A major change, compared to our previous work [5], concerns the treatment of CO diffusion between cells. To study this type of diffusion we adopted a similar model developed by Pavlenko *et al.* in the context of CO oxidation on nanoscale Pt facets [26]. In contrast to our case the facets there exhibited different orientations and hence a different reactivity.

(iv) CO(ads) can diffuse at a finite rate from each cell to empty sites on the adjacent cells. CO(ads) would hop across a common imaginary edge of length $L=\sqrt{A}$ to adjacent empty sites at rate h (microscopic hop rate or coupling parameter). The diffusion is mimicked by the transition of CO(ads) from one cell to another at rate (in molecules per unit time) $h'N_{\mathrm{CO},i}$ times the probability that a site is empty in the other cells, where $h'=h/L$.

We choose $p_{\mathrm{CO}}+p_{\mathrm{O}_2}=k=1$, which sets the time scale. Finally, the system is controlled by the partial pressure p_{CO}, the desorption rate d, the coupling parameter h, and the number of adsorption sites A. The model is still simplistic. It does not support oscillatory kinetics, but it describes the bistability observed in experiment [19,27–29].

When $h=0$, previous studies using KMC and ODE reveal bistability in this model for $d<d_C$, where d_C corresponds to a cusp bifurcation point. Two stable kinetic stationary states coexist in parameter space for a range of $p_{\mathrm{CO}}^{-}<p_{\mathrm{CO}}<p_{\mathrm{CO}}^{+}$. On the active stationary state the surface is predominantly oxygen covered. On the inactive stationary state a high CO coverage inhibits O_2 adsorption and hence poisons the reaction. These stable states are connected by an unstable state producing an S-shaped plot of steady state coverage versus p_{CO}. For this model $d_C=0.048$ and $p_{\mathrm{CO}}^{C}=0.40$ [5,15,16]. Here, we use the multistable behavior described above as a prototype of bistability inside each cell.

III. REACTION-DIFFUSION MASTER EQUATION

The master equation describes the PDF of populations in a chemical reaction [30]. Normally, these master equations consider a global description of fluctuations in the sense that the system is treated as if it remained homogeneous. Of course, this description breaks down if we consider high pressure conditions. To obtain an adequate master equation formulation of the reaction diffusion system for CO oxidation, the cells of side length L are considered as well mixed and smaller than the diffusion length. We assume infinite diffusion of CO molecules inside a cell, and diffusion events between cells are considered to be much more frequent than chemical reactions. The state of the system is described by the probability distribution $P(N_{\mathrm{CO},i},N_{\mathrm{O},i};t)$ of finding a set of populations $\mathbf{Z}=\{N_{\mathrm{CO},i},N_{\mathrm{O},i}\}$, with $i=1,\ldots,M$ denoting the number of cells. Finally the PDF is governed by the following RDME [20,31–34]:

$$\frac{dP(\mathbf{Z};t)}{dt}=\frac{dP^{\mathrm{reac}}}{dt}+\frac{dP^{\mathrm{diff}}}{dt}. \tag{1}$$

The reaction and diffusion terms of this equation will be derived in the following subsections.

A. Reaction jump Markov processes

The transition rates $W_\rho^i(N_{\mathrm{CO},i},N_{\mathrm{O},i})$ and population changes of the particle number of carbon monoxide ($N_{\mathrm{CO},i}$) and oxygen ($N_{\mathrm{O},i}$) are

$$W_1^i(N_{\mathrm{CO},i}/N_{\mathrm{CO},i}+1)=p_{\mathrm{CO}}(A-N_{\mathrm{CO},i}-N_{\mathrm{O},i}),$$

$$W_2^i(N_{\mathrm{CO},i}/N_{\mathrm{CO},i}-1)=dN_{\mathrm{CO},i},$$

$$W_3^i(N_{\mathrm{O},i}/N_{\mathrm{O},i}+2)=2p_{\mathrm{O}_2}S_A^i(N_{\mathrm{CO},i},N_{\mathrm{O},i},A),$$

$$W_4^i(N_{\mathrm{CO},i},N_{\mathrm{O},i}/N_{\mathrm{CO},i}-1,N_{\mathrm{O},i}-1)=\frac{4kN_{\mathrm{O},i}N_{\mathrm{CO},i}}{(A-N_{\mathrm{O},i})}.$$

We require $0<N_{\mathrm{CO},i}+N_{\mathrm{O},i}\leq A$, where a small number of adsorption sites A produces high coverage fluctuations. The term $N_{\mathrm{CO},i}/(A-N_{\mathrm{O},i})$ in $W_4^i(N_{\mathrm{CO},i},N_{\mathrm{O},i})$ assumes that inside a cell each site adjacent to an O(ads) is occupied randomly by CO(ads).

$S_A^i(N_{\mathrm{CO},i},N_{\mathrm{O},i},A)$ is the normalized sticking probability for oxygen, i.e., the probability of finding two next NN empty sites with all six NN sites not occupied by oxygen (eight-site rule) [3,16]. This term can be written as

$$S_A^i(N_{\mathrm{CO},i},N_{\mathrm{O},i},A)=A\frac{(A-N_{\mathrm{CO},i}-N_{\mathrm{O},i})^2(A-2N_{\mathrm{O},i})^8}{(A-N_{\mathrm{O},i})^{10}}. \tag{2}$$

As in previous works, the reaction part of the more general RDME is expressed in the following way:

$$\frac{dP^{\mathrm{reac}}}{dt}=\sum_{i=1}^{M}\sum_{\rho=1}^{4}[W_\rho^i(\mathbf{Z}-\mathbf{v}_\rho/\mathbf{Z})P(\mathbf{Z}-\mathbf{v}_\rho;t)-W_\rho^i(\mathbf{Z}/\mathbf{Z}-\mathbf{v}_\rho)P(\mathbf{Z};t)], \tag{3}$$

where the vectors $\mathbf{v}_\rho=\{v_\rho^n\}_{n=1}^2$ are the stoichiometric vectors.

It can be shown that in the macroscopic limit of large reacting surfaces and at low pressures, this master equation reproduces the deterministic predictions [5,18,19].

B. Diffusion random walk

In order to model diffusion we assume that each absorbed CO molecule can do a random walk between adjacent cells. Like the reaction part, one can construct the transition probabilities [31]:

$$W_5^i(N_{\mathrm{CO},i}/N_{\mathrm{CO},i}-1)=\frac{h'}{2s}N_{\mathrm{CO},i}\sum_l(1-\theta_{\mathrm{CO},i+l}-\theta_{\mathrm{O},i+l}),$$

$$W_6^i(N_{\mathrm{CO},i}/N_{\mathrm{CO},i}+1)=\frac{h'}{2s}(1-\theta_{\mathrm{CO},i}-\theta_{\mathrm{O},i})\sum_l N_{\mathrm{CO},i+l}.$$

The sum l runs over the first nearest neighbors of the cell i, and s represents the space dimension. $\theta_{\mathrm{CO},i}$ and $\theta_{\mathrm{O},i}$ are $N_{\mathrm{CO},i}/A$ and $N_{\mathrm{O},i}/A$, respectively. The factors in $W_5^i(N_{\mathrm{CO},i}/N_{\mathrm{CO},i}-1)$ simply represent the transition of CO(ads) from one cell to another at a rate (in molecules per unit time) $h'N_{\mathrm{CO},i}$ times the probability that a site is empty in the first nearest neighbor cells, where $h'=h/L$. $W_6^i(N_{\mathrm{CO},i}/N_{\mathrm{CO},i}+1)$ is interpreted in the same way. Now one can write the diffusion term of the RDME as

$$\frac{dP^{\mathrm{diff}}}{dt}=\sum_{i=1}^{M}\sum_{\rho=5}^{6}[W_\rho^i(N_{\mathrm{CO},i}-1/N_{\mathrm{CO},i})P(N_{\mathrm{CO},i}-1,N_{\mathrm{CO},i+l}+1;t)-W_\rho^i(N_{\mathrm{CO},i})P(N_{\mathrm{CO},i};t)]. \tag{4}$$

Notice that, as cell area is increased, we have less and less effect from diffusion. In the same way the diffusion dominates over the reaction part for small areas. This interplay between diffusion and reaction is a direct consequence of the reaction and diffusion transition probabilities which depend on L in different ways.

The coarse-grained description of our RDME is valid when CO molecules inside each cell are considered to be candidates for a reactive collision, and if the diffusion between cells occurs much more frequently than chemical reactions. This description provides a simple generalization of deterministic reaction-diffusion equations. If one is interested in stochastic effects, it is also possible to consider a reaction-diffusion Langevin equation (a deterministic reaction-diffusion equation plus a random term) which can be derived directly from the stochastic discrete model [31]. However, contrary to the Langevin approach, the RDME used here provides a mechanistic view of the dynamics at the molecular level [30].

IV. WEISS MEAN-FIELD APPROXIMATION

We begin with considering the traditional Weiss mean-field approach from the theory of equilibrium critical phenomena [20,35,36]. In analogy with many-body theory one can expect that each cell in this approximation would interact with an averaged environment. It is well known that mean-field theory gives a rough qualitative picture of the phase transition in systems of lower dimensionality, but it is not quantitatively correct. Nevertheless, we expect from the wealth of experience in equilibrium phase transitions that mean-field theories will be essentially exact in four or more dimensions [37]. In this approximation, one neglects the correlation between neighboring cells. Basically, the nearest-neighbor interaction is replaced by a global interaction through an average field. Here, $(1/2s)\Sigma_l(1-\theta_{\mathrm{CO},i+l}-\theta_{\mathrm{O},i+l})$ and $(1/2s)\Sigma_l N_{\mathrm{CO},i+l}$ are replaced with $[1/(M-1)]\Sigma_{j=1,j\neq i}^{M}(1-\theta_{\mathrm{CO},j}-\theta_{\mathrm{O},j})$ and $[1/(M-1)]\Sigma_{j=1,j\neq i}^{M}N_{\mathrm{CO},j}$, respectively. The cells are supposed to interact all to all throughout the global coupling.

If one considers the case that the number of cells, M, goes to infinity, one can postulate

$$\lim_{M\to\infty}\frac{1}{M-1}\sum_{j=1,j\neq i}^{M}(1-\theta_{\mathrm{CO},j}-\theta_{\mathrm{O},j})=(1-\theta_{\mathrm{CO}}^{m}-\theta_{\mathrm{O}}), \quad (5)$$

$$\lim_{M\to\infty}\frac{1}{M-1}\sum_{j=1,j\neq i}^{M}N_{\mathrm{CO},j}=N_{\mathrm{CO}}^{m}. \quad (6)$$

In this limit the cells have identical evolution given by the following transition probabilities:

$$W_1(N_{\mathrm{CO}}/N_{\mathrm{CO}}+1)=p_{\mathrm{CO}}(A-N_{\mathrm{CO}}-N_{\mathrm{O}}),$$

$$W_2(N_{\mathrm{CO}}/N_{\mathrm{CO}}-1)=dN_{\mathrm{CO}},$$

$$W_3(N_{\mathrm{O}}/N_{\mathrm{O}}+2)=2p_{\mathrm{O}_2}S_A(N_{\mathrm{CO}},N_{\mathrm{O}},A),$$

$$W_4(N_{\mathrm{CO}},N_{\mathrm{O}}/N_{\mathrm{CO}}-1,N_{\mathrm{O}}-1)=\frac{4kN_{\mathrm{O}}N_{\mathrm{CO}}}{(A-N_{\mathrm{O}})},$$

$$W_5(N_{\mathrm{CO}}/N_{\mathrm{CO}}-1)=h'N_{\mathrm{CO}}(1-\theta_{\mathrm{CO}}^{m}-\theta_{\mathrm{O}}),$$

$$W_6(N_{\mathrm{CO}}/N_{\mathrm{CO}}+1)=h'(1-\theta_{\mathrm{CO}}-\theta_{\mathrm{O}})N_{\mathrm{CO}}^{m}.$$

Because oxygen does not diffuse and the sticking probability is identical in all cells, we eliminate the index i from $N_{\mathrm{O},i}$. We also introduce the order parameter $N_{\mathrm{CO}}^{m}=A\theta_{\mathrm{CO}}^{m}$, which is defined by the self-consistent equation

$$\beta(N_{\mathrm{CO}}^{m})=N_{\mathrm{CO}}^{m}=\sum_{N_{\mathrm{CO}},N_{\mathrm{O}}}N_{\mathrm{CO}}P^{\mathrm{st}}(N_{\mathrm{CO}},N_{\mathrm{O}},N_{\mathrm{CO}}^{m}). \quad (7)$$

Note that $N_{\mathrm{CO}}^{m}=A\theta_{\mathrm{CO}}^{m}$ is the average value of CO molecules inside each cell. This first moment or mean value is an order parameter that determines the occurrence of a phase transition. The multiple solutions of this complicated equation reflect the possibility of bifurcations that break the ergodicity associated with the presence of a true phase transition [35]. Finally, we have a mean-field coupling master equation (MFCME) without spatial correlations,

$$\frac{dP(\mathbf{Z},N_{\mathrm{CO}}^{m};t)}{dt}=\frac{dP^{\mathrm{reac}}}{dt}+\frac{dP^{\mathrm{MF}}}{dt}, \quad (8)$$

where $\mathbf{Z}=\{N_{\mathrm{CO}},N_{\mathrm{O}}\}$.

The challenge now is to solve this MFCME in order to obtain the stationary probability distribution $P^{\mathrm{st}}(\mathbf{Z},N_{\mathrm{CO}}^{m})$, and then to solve Eq. (7) in order to investigate the possibility of a phase transition in our model. Like other nonequilibrium problems related to a noise-induced phase transition, $P^{\mathrm{st}}(\mathbf{Z},N_{\mathrm{CO}}^{m})$ is not available in general [38]. At this point, we are forced to introduce a new approximation: The so-called adiabatic elimination of fast variables.

V. ADIABATIC ELIMINATION OF OXYGEN

Theoretical methods for the adiabatic elimination of fast-relaxing variables from master equations have received a great deal of interest in past years [39–41]. This is motivated partially by the fact that in most cases it is difficult or impossible to solve this equation. It is also known that for large complicated chemical networks, model reduction often provides a way to efficient computational methods. These techniques assume that fast variables are in a quasisteady state with respect to the remaining slow variables. If the quasisteady state distributions conditioned on the slow variables can be determined, then they can be used to eliminate the fast variables. Under some conditions one can approximate the corresponding fast variable using Langevin or deterministic equations [42].

As shown recently, in catalytic CO oxidation N_{O} is the fast variable and N_{CO} is the slow one. This was reported first by Bär *et al.* in a deterministic model [43]. More recently, we observed that the same assumption can be used in a homogeneous stochastic model at low pressure [5]. Finally, new transition probabilities can be constructed after adiabatic elimination of oxygen.

For the reaction part we use

$$\widetilde{W}_1(N_{\mathrm{CO}}/N_{\mathrm{CO}}+1)=p_{\mathrm{CO}}(A-N_{\mathrm{CO}}-\widetilde{N}_{\mathrm{O}}),$$

$$\widetilde{W}_2(N_{\mathrm{CO}}/N_{\mathrm{CO}}-1)=dN_{\mathrm{CO}},$$

$$\widetilde{W}_3(N_{\mathrm{CO}}/N_{\mathrm{CO}}-1)=\frac{4k\widetilde{N}_{\mathrm{O}}N_{\mathrm{CO}}}{(A-\widetilde{N}_{\mathrm{O}})},$$

and for the diffusion random walk

$$\widetilde{W}_4(N_{\mathrm{CO}}/N_{\mathrm{CO}}-1)=h'N_{\mathrm{CO}}(1-\theta^m_{\mathrm{CO}}-\widetilde{\theta}_{\mathrm{O}}),$$

$$\widetilde{W}_5(N_{\mathrm{CO}}/N_{\mathrm{CO}}+1)=h'(1-\theta_{\mathrm{CO}}-\widetilde{\theta}_{\mathrm{O}})N^m_{\mathrm{CO}}.$$

The transition probability associated with the oxygen adsorption is eliminated from the stochastic description. Note that the notation is changed from N_{O} to $\widetilde{N}_{\mathrm{O}}$ in order to emphasize that oxygen has been adiabatically eliminated.

The time scale separation between the two random variables N_{O} and N_{CO} is large enough that one can decompose the joint PDF as

$$P(N_{\mathrm{CO}},\widetilde{N}_{\mathrm{O}},N^m_{\mathrm{CO}};t)=G(N_{\mathrm{CO}},N^m_{\mathrm{CO}};t)F(\widetilde{N}_{\mathrm{O}}:N_{\mathrm{CO}};t),$$

where $F(\widetilde{N}_{\mathrm{O}}:N_{\mathrm{CO}};t)$ is the quasisteady state conditional PDF with N_{CO} kept constant. $F(\widetilde{N}_{\mathrm{O}}:N_{\mathrm{CO}};t)$ is a sharply peaked monomodal function around $\widetilde{N}_{\mathrm{O}}$. Thus $\widetilde{N}_{\mathrm{O}}=A\widetilde{\theta}_{\mathrm{O}}$ is a solution of

$$\frac{d\widetilde{\theta}_{\mathrm{O}}}{dt}=2(1-p_{\mathrm{CO}})\frac{(1-\theta_{\mathrm{CO}}-\widetilde{\theta}_{\mathrm{O}})^2(1-2\widetilde{\theta}_{\mathrm{O}})^8}{(1-\widetilde{\theta}_{\mathrm{O}})^{10}}-\frac{4\theta_{\mathrm{CO}}\widetilde{\theta}_{\mathrm{O}}}{(1-\widetilde{\theta}_{\mathrm{O}})},\tag{9}$$

for each $N_{\mathrm{CO}}=A\theta_{\mathrm{CO}}$ [5]. Note that we approximate the stochastic fast variable by using the deterministic equation corresponding to this variable. It is just an approximation, which holds true for a sharply single peaked function $F(\widetilde{N}_{\mathrm{O}}:N_{\mathrm{CO}};t)$. A generalization obviously must include higher moments, too [38].

This approximation allows us to construct a new one component nonlinear MFCME for N_{CO} alone. Considering that now $\mathbf{Z}=\{N_{\mathrm{CO}}\}$, this new master equation describes the behavior of the new probability distribution $G(N_{\mathrm{CO}},N^m_{\mathrm{CO}};t)$. In the Appendix, we derive master equations for $G(N_{\mathrm{CO}},N^m_{\mathrm{CO}};t)$ and $F(\widetilde{N}_{\mathrm{O}}:N_{\mathrm{CO}};t)$ from the master equation of $P(N_{\mathrm{CO}},\widetilde{N}_{\mathrm{O}},N^m_{\mathrm{CO}};t)$.

The new one-component MFCME can be written as

$$\frac{dG(\mathbf{Z},N^m_{\mathrm{CO}};t)}{dt}=\frac{dG^{\mathrm{reac}}}{dt}+\frac{dG^{\mathrm{MF}}}{dt}.\tag{10}$$

$G(N_{\mathrm{CO}},N^m_{\mathrm{CO}};t)$ is the PDF of one cell and its environment after neglecting the spatial correlation. This nonlinear one-component MFCME can be written in the function of the new transition probabilities in the following way:

$$\begin{aligned}\frac{dG(N_{\mathrm{CO}},N^m_{\mathrm{CO}};t)}{dt}&=H_1(N_{\mathrm{CO}}-1)G(N_{\mathrm{CO}}-1,N^m_{\mathrm{CO}};t)\\&\quad-H_1(N_{\mathrm{CO}})G(N_{\mathrm{CO}},N^m_{\mathrm{CO}};t)\\&\quad+H_2(N_{\mathrm{CO}}+1)G(N_{\mathrm{CO}}+1,N^m_{\mathrm{CO}};t)\\&\quad-H_2(N_{\mathrm{CO}})G(N_{\mathrm{CO}},N^m_{\mathrm{CO}};t),\end{aligned}\tag{11}$$

where

$$H_1=\widetilde{W}_1+\widetilde{W}_5,$$

$$H_2=\widetilde{W}_2+\widetilde{W}_3+\widetilde{W}_4.$$

The probability distribution $G(N_{\mathrm{CO}},N^m_{\mathrm{CO}};t)$ approaches a stationary shape, which includes macroscopic transitions between the stable states of the deterministic approach. The final shape of $G(N_{\mathrm{CO}},N^m_{\mathrm{CO}};t)$ is in agreement with the solution $dG^{\mathrm{st}}(N_{\mathrm{CO}},N^m_{\mathrm{CO}})/dt=0$, and vanishing probability flux. In this case, detailed balance holds and one finds

$$H_1(N_{\mathrm{CO}}-1)G^{\mathrm{st}}(N_{\mathrm{CO}}-1,N^m_{\mathrm{CO}})=H_2(N_{\mathrm{CO}})G^{\mathrm{st}}(N_{\mathrm{CO}},N^m_{\mathrm{CO}}),\tag{12}$$

and subsequently

$$G^{\mathrm{st}}(N_{\mathrm{CO}},N^m_{\mathrm{CO}})=\prod_{N=1}^{N_{\mathrm{CO}}}\frac{H_1(N-1)}{H_2(N)}\left(1+\sum_{k=1}^{A}\prod_{N=1}^{k}\frac{H_1(N-1)}{H_2(N)}\right)^{-1}.\tag{13}$$

This equation is the normalized stationary PDF for the occupation of sites with N_{CO} molecules.

After adiabatic elimination Eq. (7) can be written as

$$\beta(N^m_{\mathrm{CO}})=N^m_{\mathrm{CO}}=\sum_{N_{\mathrm{CO}},\widetilde{N}_{\mathrm{O}}}N_{\mathrm{CO}}G^{\mathrm{st}}(N_{\mathrm{CO}},N^m_{\mathrm{CO}})F^{\mathrm{st}}(\widetilde{N}_{\mathrm{O}}:N_{\mathrm{CO}}),\tag{14}$$

and considering

$$\sum_{\widetilde{N}_{\mathrm{O}}}F^{\mathrm{st}}(\widetilde{N}_{\mathrm{O}}:N_{\mathrm{CO}})=1,\tag{15}$$

the new self-consistent equation or order parameter of the system can be written as

$$\beta(N^m_{\mathrm{CO}})=N^m_{\mathrm{CO}}=\sum_{N_{\mathrm{CO}}}N_{\mathrm{CO}}G^{\mathrm{st}}(N_{\mathrm{CO}},N^m_{\mathrm{CO}}).\tag{16}$$

Note that this order parameter is the mean value of the CO coverage obtained from the PDF. In our problem two cases are possible. (i) The PDF is unique, and the order parameter has only one value. (ii) We have several monomodal PDFs and the order parameter has several solutions, one for each PDF.

VI. EVIDENCE FOR A PHASE TRANSITION

Inside each cell bistable behavior is possible, and the number of adsorption sites A is of nanoscale dimension. Thus fluctuation-induced transitions from the active to the

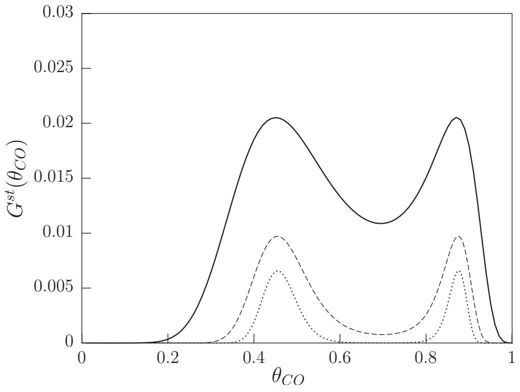

FIG. 1. Stationary probability distribution $G^{\mathrm{st}}(N_{\mathrm{CO}})$ obtained from Eq. (13) considering only the bistable behavior inside one single cell ($h=0$), with $p_{\mathrm{CO}}=0.36715$, $d=0.030$, and the number of adsorption sites $A=100$ (solid line), 400 (dashed line), and 1000 (dotted line).

inactive state and vice versa may occur. This property opens up the possibility of studying the interplay of coverage fluctuations induced by a small number of adsorption sites, and the coupling between cells.

We are only interested in the fluctuations that are induced by a small number of adsorption sites, and not in the fluctuations that occur near the cusp bifurcation point (where the mean-field approximation breaks down because the correlations become important). In this paper the pressure and the desorption rate are chosen as $p_{\mathrm{CO}}=0.36715$ and $d=0.030$, respectively. Note that this point is relatively far away from the cusp bifurcation point, which for this model in the infinite adsorption site limit is found at ($p_{\mathrm{CO}}^{C}=0.40$, $d_C=0.048$) [5]. First, we consider the case that the coupling between cells is zero and the cells are independent systems described by simple master equations which allow only global fluctuations. Inside of each cell CO molecules can diffuse infinitely fast, and this naturally produces bistability. As an example, Fig. 1 shows a typical bimodal stationary PDF for the case when $h=0$ with $A=100$, 400, and 1000. Note that, if A decreases, the transitions between the two stable states will increase. This result is in accordance with experiments of fluctuation-induced transitions in CO oxidation on a Pt field emitter tip, and with CO oxidation on Pd nanoparticles [2,4,5]. However, when the coupling parameter h increases, the CO molecules can jump from cell to cell and a RDME approach is necessary. Then it is clear that the order parameter defined by Eq. (16), which is derived from the Weiss mean-field approximation, becomes the most important variable of the model in order to study the possibility of phase transitions. A true phase transition is detected when an abrupt change in this order parameter is observed as a function of control parameters.

If the order parameter has only one solution, it is expected that the system evolves to a collective highly symmetric state. In this state of high symmetry, the cells relax to a unique mean value with only one stationary PDF. For other parameter values, multiple mean value solutions are possible and the system relaxes to a collective low symmetry state, where the cells randomly approach one or another solution depending on the initial conditions. In this case, one concludes that there are several corresponding stationary PDFs, and the mean-field theory predicts a phase transition. The latter case can be understood as a breaking of the symmetry.

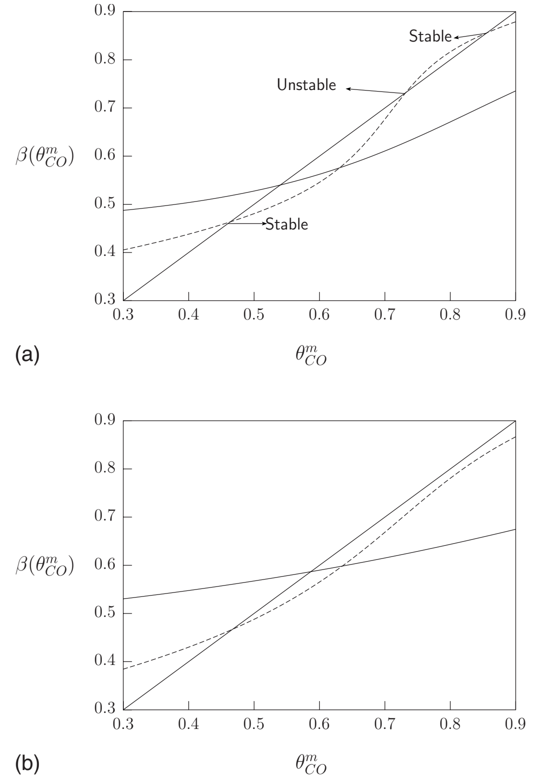

FIG. 2. Solutions of the self-consistent equation (16). The solutions are given by the intersection of $\beta(N_{\mathrm{CO}}^{m})$ with the diagonal solid line. (a) Here $A=400$, and the solid line, which corresponds to $h=0.1$, shows only one stable solution of this equation (highly symmetric state). On the other hand, the dotted line, which now corresponds to $h=2$, shows three solutions (low symmetry state). (b) In this case $A=100$, and for the whole range of h one observes only one solution (highly symmetric state). The reaction parameters are $p_{\mathrm{CO}}=0.36715$ and $d=0.030$.

Figure 2 shows a graphical representation of Eq. (16). All the self-consistently determined solutions are given by the intersection of the diagonal line with the curve $\beta(N_{\mathrm{CO}}^{m})$. In Fig. 2(a) two typical cases are shown for two values of h and with the number of adsorption sites $A=400$. For $h=0.1$ only one solution is observed (solid line). In this case a homogeneous highly symmetric state dominates. As the coupling is increased, for $h=2$ three solutions appear which represent a low symmetric state (dashed line). Figure 2(b) shows that for $A=100$ only one solution is observed for the whole range of h. Note that we plot the self-consistent equation as a function of the CO coverage.

In order to clarify these latter observations, we perform an analysis of bifurcation diagrams of N_{CO}^{m} as function of h and the corresponding stationary PDFs. Figure 3(a) shows one of these bifurcation diagrams with $A=400$. Here, one solution remains stable (the lower branch), while a new stable solution and unstable solution appear above some critical value of h. For small coupling N_{CO}^{m} is unique (case I) and one bimodal stationary PDF as in Fig. 3(b) is observed. If the

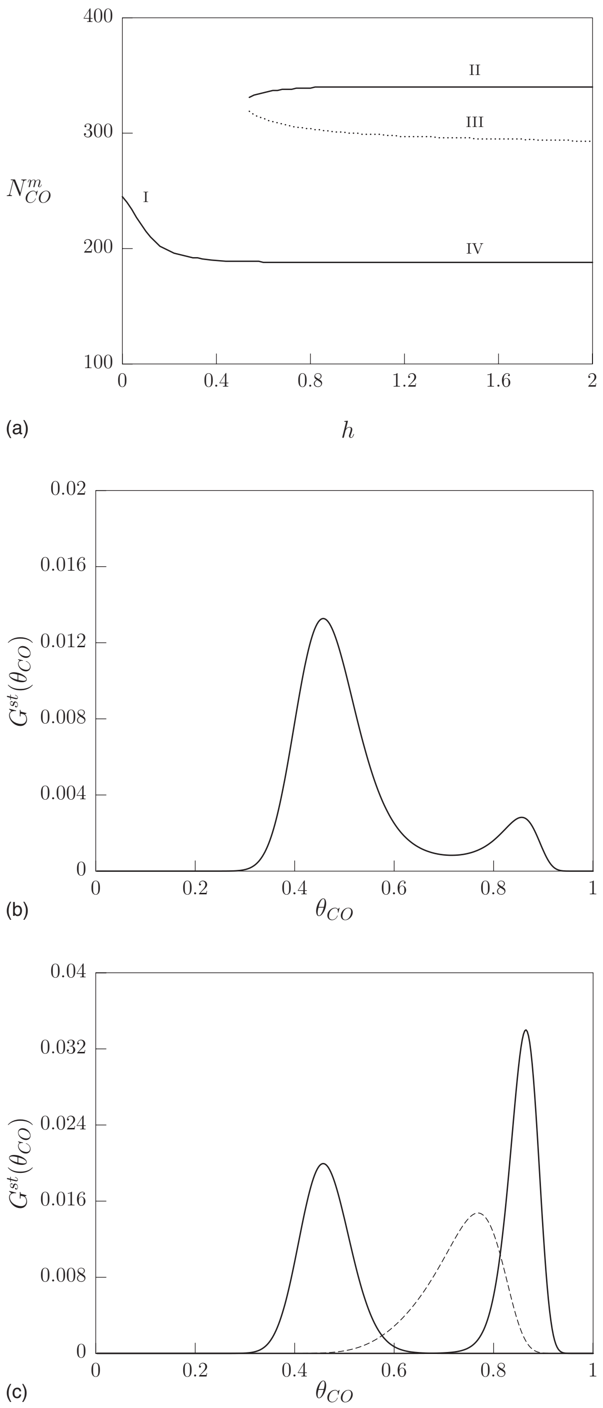

FIG. 3. Solution of Eq. (16) as a function of the coupling parameter h and the corresponding stationary probability distribution functions. (a) Here, we show the bifurcation diagram of N^m_{CO}. First, for small enough h, the model is in a state of high symmetry where only one solution is observed (case I), but above some critical value of h the model presents a low symmetry state characterized by three solutions. The two extreme solutions are stable (cases II and IV), and the intermediate one represented by the dotted line is unstable (case III). (b) Bimodal stationary probability distribution for case I. (c) Three monomodal stationary probability distributions for cases II, III, and IV. The CO pressure and desorption rate are constant with $p_{\mathrm{CO}}=0.36715$ and $d=0.030$. Each cell also has the same number of sites $A=400$.

coupling increases, the system behavior departs from that of the small coupling until a bifurcation takes place to a region where two new solutions appear (cases II and III). Here, a subset of cells may have a tiny preference to the upper solution, while the rest may have a certain preference to the lower solution, with the result that the overall behavior is not fully symmetric. In this case, the intermediate solution is unstable. These solutions, of course, correspond to three different monomodal PDFs. Figure 3(c) shows these PDFs. The PDF represented by the dotted line corresponds to the unstable solution, and it is not observed in simulations. Here one observes cells with high θ_{CO} coexisting with cells of low θ_{CO}. In Fig. 4(a), we plot the same as in Fig. 3, but now with $A=100$. From this figure it is clear that only the lower solution of Fig. 3(a) is observed and corresponds to one stable stationary PDF. Nevertheless, this PDF can change from a bimodal shape to a monomodal shape as shown in Figs. 4(b) and 4(c).

Obviously, when one decreases the cell size and increases the parameter h, the whole system behaves in a different way. This different behavior arises from the different scaling of the diffusion and reaction part of the RDME, as mentioned earlier. On a small surface the diffusion dominates, since fluctuations arising from diffusion come about because the molecules are jumping back and forth across the boundary of length L. Conversely, for larger surfaces, we find the diffusion between cells is negligible and only reaction dominates [44].

The phase diagram in the parameter space (h,A), showing only two phases as predicted by the mean-field approach, is shown in Fig 5. One region consists of two stable solutions and one unstable solution of Eq. (16) corresponding to three PDFs (low symmetry state). The second region is characterized by only one PDF corresponding to one stable solution of the order parameter (highly symmetric state).

In order to verify the analytical results, simulations have been carried out with the Gillespie algorithm [24,45]. This algorithm has received much attention in past years [46,47]. For instance, some efficient generalizations to extended systems have been introduced [48,49]. Here, in contrast to the normal algorithm, we have taken into account the adiabatic elimination of oxygen and the Weiss mean-field approximation. The computer simulations have been carried out with M or the number of cells equal to 2000. We choose appropriate initial conditions, long simulation time, and parameters as in the previous theoretical part. Figure 6(a) shows the two PDFs inside the region of low symmetry with $A=400$. In Fig. 6(b) the stationary PDF, but now with $A=100$, is shown. This result is also in accordance with the highly symmetry state predicted by analytical solutions.

VII. SUMMARY AND CONCLUSIONS

We have analyzed theoretically the interplay between internal fluctuations and diffusion in a model of the bistable CO oxidation reaction which applies to the case of a catalytic surface at high enough pressure. At higher pressure the adsorption rates grow proportionally to the pressure, the diffusion length decreases, and smaller and smaller patches of the

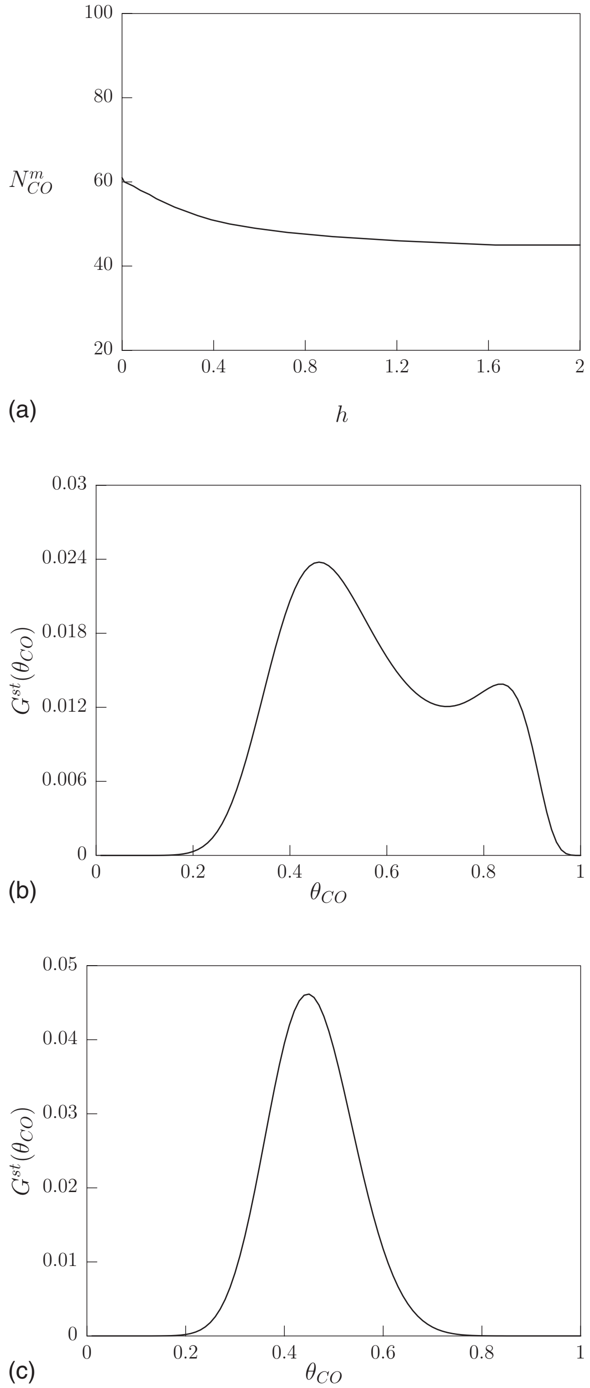

FIG. 4. The same as Fig. 3, but now with $A=100$. (a) Bifurcation diagram of N^m_{CO} as a function of h. It is clear that only the lower solution of Fig. 3(a) is physical and corresponds to one stationary probability distribution function. Figures (b) and (c) show that this probability distribution function can change from a bimodal shape to a monomodal shape.

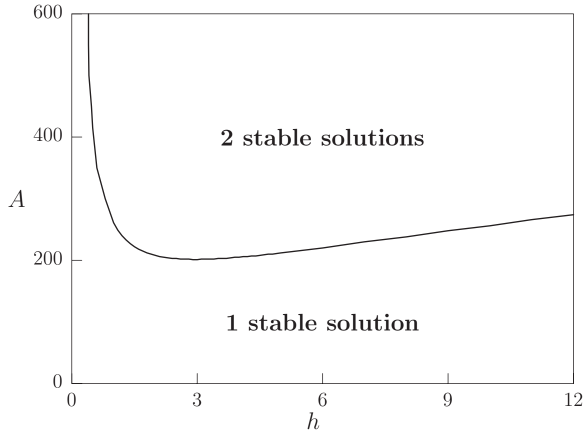

FIG. 5. Phase diagram in the (h,A) plane as predicted by the mean-field approximation, with $p_{\mathrm{CO}}=0.36715$ and $d=0.030$. The regions with different numbers of solutions clearly indicate a phase transition. In the region where one stable solution of Eq. (16) is observed, a highly symmetric homogeneous state dominates the system. On the other hand, in the region where two stable solutions of this equation are possible, a low symmetry state with a structure characterized by coexisting cells with high and low CO coverage will dominate.

surface can be regarded as well mixed. Consequently, stochastic fluctuations become important. In this publication stochastic effects are taken into account by dividing the surface into a square lattice of nanoscale cells, each containing A adsorption sites. A reaction-diffusion master equation for the probability of finding CO and oxygen coverage at a time t, that allows local fluctuations, is introduced. We are able to solve this complicated reaction-diffusion master equation after invoking the Weiss mean-field approach together with the adiabatic elimination of oxygen. This allows an estimation of the probability distribution of adsorbed CO molecules as a function of the coupling parameter h and the number of adsorption sites A. Subsequently, the phase diagram in the parameter space (h,A) is constructed. Assuming that the bistable behavior is possible inside each cell, we show that the phase diagram, as predicted by the Weiss mean-field approximation, is split into two regions. An analysis of the probability distribution shows evidence for the existence of a phase transition associated with the bifurcation of the first moment of the CO coverage. The first moment plays the role of the order parameter which characterizes this phase transition. These analytical results have been found to be in reasonable agreement with Gillespie-like Monte Carlo simulations, taking into account the adiabatic elimination of oxygen and the Weiss mean-field approximation.

It remains to verify of course the range of validity of the Weiss mean-field predictions. We underline that this approximation assumes a different molecular exchange process. Local diffusional exchange is replaced by nonlocal interaction with a large number of identical neighbors. Hence the approach used here can be seen as a first mathematical treatment to find analytic results. As several studies show [7–9,35,38], the approach often predicts qualitatively correct answers, but fails quantitatively. Therefore, also in this case the boundaries of the validity of this approach have to be determined in high dimensional numerical simulations.

It is important to emphasize that, at high pressure, temperature effects are relevant and should also be taken into account for an improved model [50]. In this high pressure regime, due to the high coverage, energetic interactions between the adspecies will play an important role which needs to be adequately described in a realistic model [51]. Our

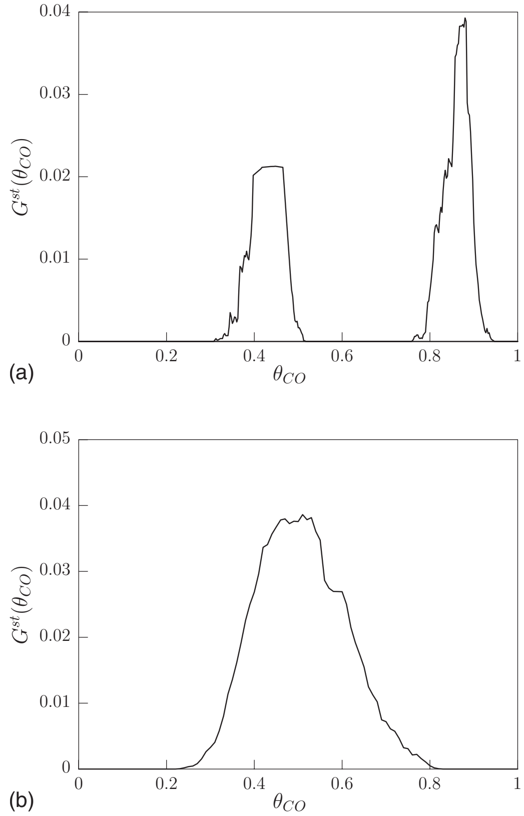

FIG. 6. Stationary probability distribution functions of one cell, obtained from the Gillespie algorithm with random initial conditions and long simulation times. (a) Here, typical stationary probability distribution functions inside the region of low symmetry for $A=400$ are shown. (b) For $A=100$, the diffusion dominates over the reaction, and a monomodal probability distribution around the mean value is obtained. This distribution is independent of the initial conditions. The Gillespie algorithm was extended in order to consider the adiabatic elimination of oxygen and the Weiss mean-field approximation. The computer simulations have been carried out with 2000 cells.

model can in principle be used to study fluctuations on inhomogeneous metal surfaces, where structural defects of such steps or impurities are present. The structural defects can be considered as small regions on the surface with different kinetic parameters coupled by CO diffusion. An interesting extention could also be to use stochastic models, like the master equation used in this paper, in order to study an array of nanoparticles coupled globally through the gas phase [52].

The results shown in this paper demonstrate that noise can play an important role in catalytic systems. This opens up new perspectives for the study of noise-induced effects because conditions with a small enough mixing area will be realized in many catalytic reactions at high pressure.

ACKNOWLEDGMENTS

M.P is supported by DAAD and FGMA. L.S.G. acknowledges Sfb 555 for financial support.

APPENDIX: ADIABATIC ELIMINATION

In this appendix we derive the one-component master equation for $G(N_{\mathrm{CO}},N^{m}_{\mathrm{CO}},t)$, using adiabatic elimination of oxygen [5].

One can partition the system into two: The fast N_{CO} and the slow $\tilde{N}_{\mathrm{O}}$ variables. Then we consider $\mathbf{Z}=\{N_{\mathrm{CO}},\tilde{N}_{\mathrm{O}}\}$, with the stoichiometric coefficients $\mathbf{v}_1=\{1,0\}$, $\mathbf{v}_2=\{-1,0\}$, $\mathbf{v}_3=\{0,2\}$, $\mathbf{v}_4=\{-1,-1\}$, $\mathbf{v}_5=\{-1,0\}$, and $\mathbf{v}_6=\{1,0\}$. From the time scale separation we have taken that $P(N_{\mathrm{CO}},\tilde{N}_{\mathrm{O}};t)=G(N_{\mathrm{CO}},N^{m}_{\mathrm{CO}};t)F(\tilde{N}_{\mathrm{O}}:N_{\mathrm{CO}};t)$, where $F(\tilde{N}_{\mathrm{O}}:N_{\mathrm{CO}};t)$ is the conditional probability for N_{CO} kept constant. Note also that we changed the notation from N_{O} to $\tilde{N}_{\mathrm{O}}$. We also require

$$\sum_{N_{\mathrm{CO}}} G(N_{\mathrm{CO}},N^{m}_{\mathrm{CO}})=1, \tag{A1}$$

$$\sum_{\tilde{N}_{\mathrm{O}}} F(\tilde{N}_{\mathrm{O}}:N_{\mathrm{CO}})=1. \tag{A2}$$

Inserting $P(N_{\mathrm{CO}},\tilde{N}_{\mathrm{O}};t)=G(N_{\mathrm{CO}},N^{m}_{\mathrm{CO}};t)F(\tilde{N}_{\mathrm{O}}:N_{\mathrm{CO}};t)$ into Eq. (8) and summing up over $\tilde{N}_{\mathrm{O}}$, we obtain

$$\begin{aligned}\frac{dG(N_{\mathrm{CO}},N^{m}_{\mathrm{CO}};t)}{dt}&=H_1(N_{\mathrm{CO}}-1)G(N_{\mathrm{CO}}-1,N^{m}_{\mathrm{CO}};t)\\&\quad-H_1(N_{\mathrm{CO}})G(N_{\mathrm{CO}},N^{m}_{\mathrm{CO}};t)\\&\quad+H_2(N_{\mathrm{CO}}+1)G(N_{\mathrm{CO}}+1,N^{m}_{\mathrm{CO}};t)\\&\quad-H_2(N_{\mathrm{CO}})G(N_{\mathrm{CO}},N^{m}_{\mathrm{CO}};t).\end{aligned}$$

We consider the new transition probabilities of Sec. V

$$H_1=\tilde{W}_1+\tilde{W}_5,$$

$$H_2=\tilde{W}_2+\tilde{W}_3+\tilde{W}_4,$$

with

$$\tilde{W}(N_{\mathrm{CO}})=\sum_{\tilde{N}_{\mathrm{O}}} W(\tilde{N}_{\mathrm{O}},N_{\mathrm{CO}})F(\tilde{N}_{\mathrm{O}}:N_{\mathrm{CO}}), \tag{A3}$$

given the conditional expectation of $W(\tilde{N}_{\mathrm{O}},N_{\mathrm{CO}})$.

On the other hand, the chemical master equation of the conditional probability distribution $F(\tilde{N}_{\mathrm{O}}:N_{\mathrm{CO}};t)$ with N_{CO} kept constant is given by

$$\begin{aligned}\frac{dF(\tilde{N}_{\mathrm{O}}:N_{\mathrm{CO}};t)}{dt}&=W_3(\tilde{N}_{\mathrm{O}}-2)F(\tilde{N}_{\mathrm{O}}-2:N_{\mathrm{CO}};t)\\&\quad-W_3(\tilde{N}_{\mathrm{O}})F(\tilde{N}_{\mathrm{O}}:N_{\mathrm{CO}};t)\\&\quad+W_4(\tilde{N}_{\mathrm{O}}+1)F(\tilde{N}_{\mathrm{O}}+1:N_{\mathrm{CO}};t)\\&\quad-W_4(\tilde{N}_{\mathrm{O}})F(\tilde{N}_{\mathrm{O}}:N_{\mathrm{CO}};t).\end{aligned} \tag{A4}$$

This master equation depends only on W_3 and W_4, which are derived in Sec. IV. Due to the time scale separation, $F(\tilde{N}_{\mathrm{O}}:N_{\mathrm{CO}};t)$ will quickly relax to a stationary distribution. Hence moments in the conditional transition rates become stationary as well as independent of the initial condition value $\widetilde{N}_{\mathrm{O}}$. Because $F^{\mathrm{st}}(\widetilde{N}_{\mathrm{O}}:N_{\mathrm{CO}})$ is sharply peaked and monomodal, the conditional first and higher moments are given by the stationary attractive coverage of the fast deterministic dynamic with θ_{CO} kept constant [5]. In our case, the oxygen is the fast variable, and the deterministic equation of it is given by

$$\frac{d\widetilde{\theta}_{\mathrm{O}}}{dt} = 2(1-p_{\mathrm{CO}})\frac{(1-\theta_{\mathrm{CO}}-\widetilde{\theta}_{\mathrm{O}})^2(1-2\widetilde{\theta}_{\mathrm{O}})^8}{(1-\widetilde{\theta}_{\mathrm{O}})^{10}} - \frac{4\theta_{\mathrm{CO}}\widetilde{\theta}_{\mathrm{O}}}{(1-\widetilde{\theta}_{\mathrm{O}})}. \tag{A5}$$

This last equation can be obtained from a standard pair or Kirkwood approximation [16].

[1] I. Chorkendorff and J. W. Niemantsverdriet, *Concepts of Modern Catalysis and Kinetics* (VCH, Weinheim, 2003).
[2] Y. Suchorski, J. Beben, E. W. James, J. W. Evans, and R. Imbihl, Phys. Rev. Lett. **82**, 1907 (1999).
[3] Y. Suchorski, J. Beben, R. Imbihl, E. W. James, Da-Jiang Liu, and J. W. Evans, Phys. Rev. B **63**, 165417 (2001).
[4] V. Johánek, M. Laurin, A. W. Grant, B. Kasemo, C. R. Henry, and J. Libuda, Science **304**, 1639 (2004).
[5] M. Pineda, R. Imbihl, L. Schimansky-Geier, and Ch. Zülicke, J. Chem. Phys. **124**, 044701 (2006).
[6] J. Starke, C. Reichert, M. Eiswirth, H. H. Rotermund, and G. Ertl, Europhys. Lett. **73**, 820 (2006).
[7] J. Garcia-Ojalvo and J. M. Sancho, *Noise in Spatially Extended Systems* (Springer-Verlag, New York, 1999).
[8] B. Lindner, J. Garcia-Ojalvo, A. Neiman, and L. Schimansky-Geier, Phys. Rep. **392**, 321 (2004).
[9] M. Löcher, *Noise Sustained Patterns* (World Scientific, Singapore, 2003).
[10] L. Yang, Z. Hou, and H. Xin, J. Chem. Phys. **109**, 2002 (1998).
[11] L. Yang, Z. Hou, B. Zhou, and H. Xin, J. Chem. Phys. **109**, 6456 (1998).
[12] I. Derényi, C. Lee, and A. L. Barabási, Phys. Rev. Lett. **80**, 1473 (1998).
[13] Y. Hayase, S. Wehner, J. Küppers, and H. R. Brand, Phys. Rev. E **69**, 021609 (2004).
[14] P. Hoffmann, S. Wehner, D. Schmeisser, H. R. Brand, and J. Küppers, Phys. Rev. E **73**, 056123 (2006).
[15] M. Tammaro, M. Sabella, and J. W. Evans, J. Chem. Phys. **103**, 10277 (1995).
[16] E. W. James, C. Song, and J. W. Evans, J. Chem. Phys. **111**, 6579 (1999).
[17] M. Tammaro and J. W. Evans, J. Chem. Phys. **108**, 762 (1998).
[18] D. J. Liu and J. W. Evans, J. Chem. Phys. **117**, 7319 (2002).
[19] C. Reichert, J. Starke, and M. Eiswirth, J. Chem. Phys. **115**, 4829 (2001).
[20] M. Malek-Mansour and G. Nicolis, J. Stat. Phys. **13**, 197 (1975).
[21] M. M. de Oliveira and R. Dickman, Physica A **343**, 525 (2004).
[22] D. T. Gillespie, J. Phys. Chem. **81**, 2340 (1977).
[23] C. T. Campbell, G. Ertl, G. Kuipers, and J. Segner, J. Chem. Phys. **73**, 5862 (1980).
[24] R. Imbihl and G. Ertl, Chem. Rev. (Washington, D.C.) **95**, 697 (1995).
[25] S. L. Chang and P. A. Thiel, Phys. Rev. Lett. **59**, 296 (1987).
[26] N. Pavlenko, R. Imbihl, J. W. Evans, and Da-Jiang Liu, Phys. Rev. E **68**, 016212 (2003).
[27] E. S. Kurkina and N. L. Semedyaeva, Surf. Sci. Lett. **558**, 122 (2004).
[28] Y. Suchorski, W. Drachsel, V. V. Gorodetskii, V. K. Medvedev, and H. Weiss, Surf. Sci. **600**, 1579 (2006).
[29] H. Rosé, H. Hempel, and L. Schimansky-Geier, Physica A **206**, 421 (1994).
[30] N. G. van Kampen, *Stochastic Processes in Physics and Chemistry* (North-Holland, Amsterdam, 1987).
[31] M. Hildebrand and A. S. Mikhailov, J. Phys. Chem. **100**, 19089 (1996).
[32] F. Baras and M. M. Mansour, Phys. Rev. E **54**, 6139 (1996).
[33] M. V. Velikanov and R. Kapral, J. Chem. Phys. **109**, 281 (1998).
[34] J. Gorecki, A. L. Kawczyński, and B. Nowakowski, J. Phys. Chem. A **103**, 3200 (1999).
[35] C. Van den Broeck, J. M. R. Parrondo, J. Armero, and A. Hernández-Machado, Phys. Rev. E **49**, 2639 (1994).
[36] M. Morillo, J. Gómez-Ordonez, and J. M. Casado, Phys. Rev. E **52**, 316 (1995).
[37] M. DelleDonne and P. Ortoleva, J. Stat. Phys. **18**, 319 (1978).
[38] R. Kawai, X. Sailer, L. Schimansky-Geier, and C. Van den Broeck, Phys. Rev. E **69**, 051104 (2004).
[39] J. A. M. Janssen, J. Stat. Phys. **57**, 171 (1989).
[40] M. O. Vlad and A. Pop, Physica A **155**, 276 (1989).
[41] E. L. Haseltine and J. B. Rawlings, J. Chem. Phys. **123**, 164115 (2005).
[42] K.-H. Chiam, C. M. Tan, V. Bhargava, and G. Rajagopal, Phys. Rev. E **74**, 051910 (2006).
[43] M. Bär, Ch. Zülicke, M. Eiswirth, and G. Ertl, J. Chem. Phys. **96**, 8595 (1992).
[44] C. W. Gardiner, *Handbook of Stochastic Methods for Physics, Chemistry and the Natural Sciences* (Springer-Verlag, Berlin, 1985).
[45] W. Ebeling and L. Schimansky-Geier, Physica A **98**, 587 (1979).
[46] Y. Cao, H. Li, and L. Petzold, J. Chem. Phys. **121**, 4059 (2004).
[47] R. Erban, I. G. Kevrekidis, D. Adalsteinsson, and T. C. Elston, J. Chem. Phys. **124**, 084106 (2006).
[48] D. Bernstein, Phys. Rev. E **71**, 041103 (2005).
[49] A. Chatterjee and D. G. Vlachos, J. Chem. Phys. **124**, 064110 (2006).
[50] J. Cisternas, P. Holmes, I. G. Kevrekidis, and J. X. Li, J. Chem. Phys. **118**, 3312 (2003).
[51] D. J. Liu and J. W. Evans, J. Phys.: Condens. Matter **19**, 065129 (2007).
[52] N. V. Peskov, M. M. Slinko, and N. I. Jaeger, J. Chem. Phys. **116**, 2098 (2002).